Adaptive Position Feedback Control of Parallel Robots in the Presence of Kinematics and Dynamics Uncertainties

M. Reza J. Harandi, Ali Hassani, Mohammad Isaac Hosseini, and Hamid D. Taghirad, *Senior Member, IEEE*

***Abstract*— Uncertainties in the kinematic and dynamic parameters of a parallel robot are unavoidable. The problem is more crucial in the cases where the manipulator interacts with the environment and when it is large–scale or deployable. Furthermore, precise measurement of the velocity of the end-effector is almost inaccessible in practice. This paper addresses the above shortcomings by designing of an adaptive trajectory tracking controller with merely position feedback of joint and task space variables. Simplicity of implementation, separation of adaptation laws of dynamic and kinematic parameters, and reduction of the number of adaptation laws such that in some cases, e.g., cable-driven robots, it is identically equivalent to the number of unknown parameters are some advantages of the proposed controller. The method's efficiency is shown via implementation on a cable-driven parallel manipulator and an intraocular surgery robot.**

***Note to Practitioners*—In order to achieve a suitable response in parallel robots with traditional controllers, a precise knowledge of kinematic and dynamic parameters, together with accurate measurement of velocity, is required. In practice, these values are usually derived by robot calibration and identification. Since the system's parameters may alter or depend on external factors such as temperature, these time-consuming methods should be implemented repeatedly while the robot is out of duty. Additionally, precise velocity measurement is a prohibitive task and requires expensive instruments. This article presents a controller to address the above shortcomings. By this means, a simple adaptive controller based on position feedback is designed such that via suitable estimation of kinematic and dynamic parameters, trajectory tracking is obtained without the need for accurate initial estimates of the parameters. The proposed method has a number of advantages, including separation of the adaptation laws of kinematic parameters and dynamic parameters, simple representation of the Jacobian matrix in regressor form, and there is no requirement for velocity feedback. Furthermore, a force distribution method is introduced for redundant robots. Hence, the proposed controller is an appropriate alternative to traditional controllers widely used in industries.**

Manuscript received 12 September 2022; revised 22 November 2022; accepted 6 January 2023. Date of publication 13 January 2023; date of current version 5 January 2024. This article was recommended for publication by Associate Editor Q. Xu and Editor J. Yi upon evaluation of the reviewers' comments. *(Corresponding author: M. Reza J. Harandi.)*

The authors are with the Advanced Robotics and Automated Systems (ARAS), Faculty of Electrical Engineering, K. N. Toosi University of Technology, Tehran 16315-1355, Iran (e-mail: jafari@email.kntu.ac.ir; hassani@email.kntu.ac.ir; mohammadisaac.hosseini@email.kntu.ac.ir; taghirad@kntu.ac.ir).

This article has supplementary downloadable material available at https://doi.org/10.1109/TASE.2023.3235895, provided by the authors.

Digital Object Identifier 10.1109/TASE.2023.3235895

***Index Terms*— Adaptive control, uncertain kinematic and dynamic, trajectory tracking, parallel robots, cable-driven robots.**

I. Introduction

ROBOTIC manipulators have played a vital role in the industry in recent decades. They improve the quality of manufacturing, reduce the cost of production and accomplish tasks that are dangerous for humans [1]. The primary generation of manipulators in the industry were serial robots that have been utilized in different fields, such as automobile manufacturing companies, due to their simple structure and large workspace [2]. For applications that high precision or relatively heavy load capacity per robot weight is required, parallel robots are a better alternative [3]. In parallel robots, there are some kinematic chains connecting the base to the end-effector [4]. Due to this structure, they are suitable for various applications such as material handling, medical fields, satellite antennas, etc. [5]. Since parallel robots suffer from confined workspace, cable-driven parallel manipulators (CDPM) were developed whose workspace may be as large as the size of a stadium [6].

Despite several advantages of CDPMs that make them suitable for different applications such as video capturing, rescue services, rehabilitation, etc. [7], their actuators can merely apply tensile forces due to cable-driven structure [8]. Note that although parallel manipulators are well-known for their high precision, suitable performance is achievable only if a precise model of the robot is available. Unfortunately, usually the kinematic and dynamic parameters are not known precisely. Additionally, these parameters may be changed for different payloads, and also over time. The problem is more crucial when it is almost impossible to measure the velocity of the end-effector. In this paper, these issues are considered, and a general practical method is proposed.

Popular methods to deal with the problem of uncertain parameters are calibration and identification. These procedures, which are usually performed in an offline manner, are typically categorized into kinematic [9] and dynamic [10] calibration. Unfortunately, since the system's parameters may alter over time, these time-consuming methods should be implemented repeatedly. Furthermore, they pose a significant threat when the parameters depend on environmental conditions such as temperature or payload.

1545-5955 © 2023 IEEE. Personal use is permitted, but republication/redistribution requires IEEE permission.
See https://www.ieee.org/publications/rights/index.html for more information.

Authorized licensed use limited to: University of York. Downloaded on April 06,2025 at 12:25:52 UTC from IEEE Xplore. Restrictions apply.

Another method to tackle this problem is a flexible controller design. Adaptive control is a well–developed approach to address such problems through online estimation of the parameters [11]. In contrast to the previous methods, since parameters estimation is performed in an online manner, adaptive control does not suffer from the aforementioned shortcomings. In this method, typically the dynamic formulation is expressed in a regressor form, and a vector of unknown parameters denoted by θ is estimated through suitable adaptation laws. Note that mostly the dimension of this vector is larger than the number of unknown parameters. A class of adaptive controllers, which are called indirect adaptive control, are based on online identification of the parameters. In this case, a suitable performance is obtained if the estimation of θ converges to its actual values. This is ensured if the control inputs are persistently exciting (PE); see also the recent achievements in [12]. Model reference adaptive system (MRAS) is another class in which the control goal is attained without exact estimation of the parameters. Clearly, cases where it is possible to design an MRAS, are more efficient than the cases where indirect adaptive control could be designed.

The design of adaptive controllers with respect to dynamical parameters for serial and parallel manipulators has been studied well in literature; see, for example, [13], [14], and [15]. Furthermore, this topic has been taken into account in the case of CDPMs [16], [17], [18], [19]. The main idea of these articles is inspired by the well-known Slotine and Li controller [20] that ensures asymptotic trajectory tracking even though the parameters may not be estimated correctly. Note that in these works, it has been assumed that the robot's velocity is available for feedback. Furthermore, some researchers have concentrated on adaptive controller design in the presence of uncertainties in kinematic and dynamic parameters. In [21], an adaptive tracking controller for a 6-DOF serial robot based on the unit quaternion representation has been designed. The design of an adaptive controller for serial robots based on the expression of a phrase related to the inverse of the Jacobian matrix in regressor form has been studied in [22]. The drawbacks of these works are the complexity of controller design and also merging of the kinematic and dynamic parameters. One decade later, Wang in [23] improved the results and proposed a new controller with separate adaptation laws for unknown dynamic and kinematic parameters. Notice that in the last three mentioned works, it is assumed that the Jacobian matrix is square, and thus, it is invertible without having a null space. For the case of parallel robots, since the structure of the Jacobian matrix is different, i.e., it typically contains fractional terms, and also the equations of motion are directly expressed in the task space, the method of coping with the problem differs.

Recently, a few studies have been accomplished to address the case of parallel robots. In [24], an adaptive trajectory tracking controller has been designed where the number of adaptation laws is excessively high. To improve this work, [25] proposed an adaptive controller with dynamic feedback that the number of adaptation laws are reduced. Adaptive control of CDPMs with uncertain kinematics and dynamics has been reported in [26] and its results have been analyzed in [25]. The drawbacks of these works are the excessive number of adaptation laws and the complexity of the controller. Additionally, precise measurement of velocity is not common in robotic manipulators. Some articles have addressed this problem for serial robots and cranes; see, for example, [27], [28], and [29]. However, it seems that trajectory tracking without velocity feedback has not been studied heretofore for parallel robots. Note that based on the knowledge of authors, so far, an adaptive tracking controller concerning dynamic and kinematic parameters has not been studied in the literature for any type of manipulator with merely position feedback of joint and task space.

In this paper, we concentrate on tracking controller design for parallel mechanisms in the presence of uncertain kinematic and dynamic properties with merely position feedback. For this purpose, invoking [24], [25], a new representation of the Jacobian matrix in a regressor form is presented such that the number of kinematic adaptation laws is reduced, and therefore, the controller design is simplified. Then, by suitable definition of the adaptation laws of kinematic parameters and dynamic parameters, trajectory tracking is guaranteed via the Lyapunov direct method. The novelties and contributions of this paper together with the properties of the proposed controller are summarized as follows.

(1) Separation of adaptation laws of kinematic and dynamic parameters. In spite of previous works such as [24] and [25] that a complex controller with a large number of adaptation laws for the augmented vectors of unknown variables has been reported; in this paper, a simple control law is designed such that the adaptation laws of kinematic and dynamic parameters are isolated. This property leads to a practical controller that may be implemented easily in different situations, such as industrial robots.

(2) No requirement for velocity feedback. Notwithstanding all the previous works on this topic, the proposed controller merely needs the position feedback of joint and task space. This property essentially simplifies the implementation of the controller in practice where accurate measurement of velocity is inaccessible. Note that such a controller has not been developed for serial and parallel robots.

(3) Reduction of estimations for kinematic parameters. Over-parametrization is a common drawback of indirect adaptive controllers. It leads to an increase in the number of columns of regressor matrix that needs a higher-order PE signal for correct estimation. Additionally, over-parametrization makes the controller design more sophisticated. Here, we simplify the representation of kinematic parameters in regressor form which leads to the reasonable number of adaptation laws such that in some cases, they may be equal to the number of unknown parameters. This property may also lead to the correct parameters' estimation; see Remark 3 for more details.

(4) Utilizing the right kernel of the Jacobian matrix in redundant robots. As explained before, CDPMs are mostly designed redundantly and positive tension in cables is ensured by force distribution using the right kernel of the Jacobian matrix. On the contrary to [24] and [25] in which the null space has not been considered and its consideration led to

Authorized licensed use limited to: University of York. Downloaded on April 06,2025 at 12:25:52 UTC from IEEE Xplore. Restrictions apply.

complexity, in this paper, this issue is incorporated in the design without intricacy of stability analysis.

(5) Enhancing the results. As it will be shown in section IV via implementation of the proposed controller on two different types of parallel robots and comparison with previous methods, the results of the proposed method are shown to be superior than that of available methods considering different error indices.

II. Kinematics and Dynamics Formulation

Consider a n-DOF parallel mechanism with $m \geq n$ actuators. The dynamic equations are [25]

$$M(X)\ddot{X} + C(X, \dot{X})\dot{X} + G(X) + F_v\dot{X} = J^T(X)u, \quad (1)$$

in which $X, \dot{X} \in \mathbb{R}^n$ are the position and velocity of end-effector, respectively, $M = M^T \in \mathbb{R}^{n\times n}$ is positive definite inertia matrix, $C \in \mathbb{R}^{n\times n}$ denotes the Coriolis and centrifugal matrix, $G(X)$ is gravitational forces/torques and F_v is positive semi-definite matrix of coefficients of viscous friction (VF). $J(X) \in \mathbb{R}^{m\times n}$ is the Jacobian matrix, and $u \in \mathbb{R}^m$ is the control input. Note that similar to a number of articles such as [30] and [31], for simplicity, merely VF is considered in the model. Equation (1) has some useful properties that are listed as follows [24], [32, ch. 5].

p1. The matrix $\dot{M} - 2C$ is skew-symmetric, i.e., $\eta^T(\dot{M} - 2C)\eta = 0$ with $\eta \in \mathbb{R}^n$ being an arbitrary vector.

p2. The matrix $C(X, \dot{X})$ has the following properties:

$$\begin{aligned} C(\alpha, \beta)\gamma &= C(\alpha, \gamma)\beta, \\ C(\alpha, \beta + \gamma) &= C(\alpha, \beta) + C(\alpha, \gamma), \\ \|C(\alpha, \beta)\gamma\| &\leq \kappa_c\|\beta\|\|\gamma\|. \end{aligned} \quad (2)$$

p3. The coefficients matrix F_v satisfies the following inequality:

$$0 \leq f_{v_{min}} \leq \|F_v\| \leq f_{v_{max}}. \quad (3)$$

p4. The dynamical terms in (1) may be expressed in regressor form. Therefore,

$$\begin{aligned} &M(X)\xi_1 + C(X, \dot{X})\xi_2 + G(X) + F_v\dot{X} \\ &= Y_m(\xi_1, \xi_2, \dot{X}, X)\theta_m, \end{aligned} \quad (4)$$

in which $Y_m \in \mathbb{R}^{n\times\mathfrak{c}}$ is the regressor and $\theta_m \in \mathbb{R}^{\mathfrak{c}}$ denotes the vector of dynamical parameters.

p5. The elements of $J(X)$ are linear regarding kinematic parameters, i.e., $J_{i,j} = Y_{k_i}\Theta_{k_j}$ where $J_{i,j}$ denotes (i, j)th element of the Jacobian matrix. Based on this property, in [24] and [25], the Jacobian matrix is represented as follows:

$$J^T = Y\Theta, \qquad Y \in \mathbb{R}^{n\times l},\ \Theta \in \mathbb{R}^{l\times m}, \quad (5)$$

that leads to over-parametrization. Note that (5) is applicable to parallel robots with actuated revolute joints. Typically, the elements of the Jacobian matrix of actuated prismatic joint robots such as well-known CDPMs are fractional. In this case, we first need the following factorization:

$$J^T \triangleq J_{new}^T L^{-1}, \qquad \text{with} \quad L = \text{diag}\{l_1, \ldots, l_m\}, \quad (6)$$

in which l_is are the links' length, diag$\{\cdot\}$ denotes a diagonal matrix, and then J_{new} is representable in the form of (5). Notice that generally, the regressor and the vector (matrix) of unknown parameters do not have a physical meaning since the former contains several specified terms and the latter comprises different dynamics or kinematics parameters.

In the following section, we design an adaptive position feedback controller in the presence of uncertainties in the dynamic and kinematic parameters based on the new representation of J^T in regressor form that significantly simplifies the controller design. Note that for simplicity of the reader, the parameters of this paper are shown in Table I.

TABLE I
Table of Notations

notation	definition
X	position of end-effector
$\dot{X}$	velocity of end-effector
$M(X)$	inertia matrix
$C(X, \dot{X})$	Coriolis and centrifugal matrix
$G(X)$	gravitational forces/torques
F_v	viscous friction coefficient
$J(X)$	Jacobian matrix
u	control input
Y_m	regressor of dynamical terms
θ_m	unknown dynamical parameters
Y_{k_i}	a regressor of J^T
θ_{k_i}	an element of kinematic parameters in J^T
ν	velocity error observer
q_c	auxiliary variable
$\mathcal{J}$	inverse (pseudo-inverse) of J^T
$\bar{J}$	null space of J^T
$\aleph$	free vector
K_1, K_2	gains of the controller
δ	gain of the observer
Γ, γ_i, ρ	gains of adaptation laws

III. Adaptive Position Feedback Controller

First, presume that all the parameters of the system are known. By this means, invoking [28], the following control law is designed:

$$\begin{aligned} u = \mathcal{J}\Big(&M(X)\ddot{X}_d + C(X, \dot{X}_d)\dot{X}_d + G(X) + F_v\dot{X}_d \\ &- K_1\nu - K_2\tilde{X}\Big) + \bar{J}\aleph \end{aligned} \quad (7)$$

together with

$$\nu = q_c + \delta\tilde{X}, \quad (8a)$$

$$\dot{q}_c = -\delta q_c - \delta^2\tilde{X} \quad (8b)$$

in which $X_d(t) \in \mathcal{C}^2$ is a suitable desired trajectory which is far from singular points, $\tilde{X} = X - X_d$, K_1 and K_2 are positive

Authorized licensed use limited to: University of York. Downloaded on April 06,2025 at 12:25:52 UTC from IEEE Xplore. Restrictions apply.

definite gains, δ is a positive scalar, and q_c is an auxiliary variable. The matrices $\mathcal{J}$ and $\bar{J}$ are defined as follows

$$\begin{cases} \mathcal{J} = J^{T^{\dagger}}, \bar{J} = J^{T^{\perp}}, & n < m, \text{revolute actuated} \\ \mathcal{J} = LJ_{new}^{T^{\dagger}}, \bar{J} = LJ_{new}^{T^{\perp}}, & n < m, \text{prismatic actuated} \\ \mathcal{J} = J^{-T}, \bar{J} = 0, & n = m, \text{revolute actuated} \\ \mathcal{J} = LJ_{new}^{-T}, \bar{J} = 0, & n = m, \text{prismatic actuated} \end{cases} \tag{9}$$

where $J^{T^{\dagger}} = J(J^T J)^{-1}$ is right pseudo-inverse of J^T and $J^{T^{\perp}} \in \mathbb{R}^{m\times m-n}$ is right kernel of J^T (i.e. $J^T J^{T^{\perp}} = 0$). Furthermore, $\aleph \in \mathbb{R}^{m-n}$ is a free vector that is designed considering actuator limitations (see Remark 4 for a method of determination of $\aleph$).

Since in practice, all the parameters may be unknown, the controller (7) is modified as

$$u = \hat{\mathcal{J}}\bigg(\hat{M}(X)\ddot{X}_d + \hat{C}(X,\dot{X}_d)\dot{X}_d + \hat{G}(X) + \hat{F}_\upsilon \dot{X}_d - K_1\nu - K_2\tilde{X}\bigg) + \hat{\bar{J}}\aleph. \tag{10}$$

Note that $\hat{*}$ denotes the estimation of $*$, e.g., the estimation of M is denoted by $\hat{M}$. Based on *p4*, some terms in the above control law may be represented as follows:

$$\hat{M}(X)\ddot{X}_d + \hat{C}(X,\dot{X}_d)\dot{X}_d + \hat{G}(X) + \hat{F}_\upsilon \dot{X}_d = Y_m(\ddot{X}_d,\dot{X}_d,X)\hat{\theta}_m. \tag{11}$$

Replacing (11) in (10) yields

$$u = \hat{\mathcal{J}}\bigg(Y_m(\ddot{X}_d,\dot{X}_d,X)\hat{\theta}_m - K_1\nu - K_2\tilde{X}\bigg) + \hat{\bar{J}}\aleph. \tag{12}$$

Since substituting (12) in (1) does not lead to the omission of Jacobian transpose ($J^T\hat{\mathcal{J}} \neq I$), it is suitable to represent J^T in regressor form. As indicated in *p5*, the representation of J^T in regressor form with a matrix of unknown parameters results in excessive number of unknown parameters. To remedy this problem, a novel representation of J^T is expressed as follows:

$$J^T = \sum_{i=1}^{\ell} Y_{k_i}\theta_{k_i}, \qquad Y_{k_i} \in \mathbb{R}^{n\times m},\ \theta_{k_i} \in \mathbb{R}, \tag{13}$$

in which θ_{k_i}s are scalar. By this means, the number of θ_{k_i}s is essentially reduced such that in some cases, it may be equal to the number of unknown kinematic parameters; see section IV-A for an example.

Now, the major results of this article are presented in the following theorem. Note that for simplicity, in the sequel, we concentrate on the case of redundant parallel manipulators whose actuated joints are revolute.

Theorem 1: Consider a parallel mechanism given by (1) where the Jacobian matrix is represented as (13) with the control law (8-10) and the following adaptation laws

$$\begin{aligned} \dot{\hat{\theta}}_m &= \Gamma Y_m^T \nu + \rho\Gamma^{-1} Y_m \tanh(\tilde{X}), \\ \dot{\hat{\theta}}_{k_i} &= \gamma_i \nu^T Y_{k_i} u + \rho\gamma_i \tanh^T(\tilde{X}) Y_{k_i} u, \end{aligned} \tag{14}$$

where Γ is a positive definite matrix, γ_is are positive scalars, and $0 < \rho$ and $\epsilon := 1/\delta$ are sufficiently small. K_1 should be selected such that

$$-\kappa_c\kappa_{\dot{X}_d} + \lambda_{min}\{K_1\} + f_{\upsilon_{min}} > 0, \tag{15}$$

where κ_c was introduced in (2) and $\|\dot{X}_d\| \leq \kappa_{\dot{X}_d}$. Then, the error of trajectory tracking converges asymptotically to zero.

Proof. See Appendix. □

Notice that as explained before, for the prismatic actuated robots, first, the factorization given in (6) is required, and then J_{new}^T is represented in the form of (13). Furthermore, a conservative upper bound for ρ and ϵ is given in (59-63) and (64), respectively. Note that the observer (8) is the dirty derivative observer of velocity that is typically used in practice where causal derivative of position is utilized. In *Theorem 1*, it was proven that if the dynamic of the observer is sufficiently fast, the stability of the closed-loop system is achieved without velocity feedback.

Remark 1: As stated previously, a significant benefit of Theorem 1 in comparison with earlier methods is its simplicity of implementation. Here, similar to previous papers such as [23], [24], [25], and [26], we redesign the controller based on Slotine and Li controller [20] and assume that $\dot{X}$ is available for feedback, the control law together with adaptation laws are

$$\begin{aligned} u &= \hat{\mathcal{J}}(\hat{M}\dot{\nu} + \hat{C}\nu + \hat{G} + \hat{F}_\upsilon\dot{X} - KS) + \hat{\bar{J}}\aleph, \\ \dot{\hat{\theta}}_m &= -\Gamma Y_m^T S,, \\ \dot{\hat{\theta}}_{k_i} &= \gamma_i S^T Y_{k_i} u, \end{aligned} \tag{16}$$

in which

$$\nu = \dot{X}_d - \Pi\tilde{X}, \quad S = \dot{X} - \nu = \dot{\tilde{X}} + \Pi\tilde{X}, \tag{17}$$

and K, Π are positive definite matrices. Replacing the control law (16) in (1), yields

$$M\ddot{X} + C\dot{X} + G + F_\upsilon\dot{X} = \hat{M}\dot{\nu} + \hat{C}\nu + \hat{G} + \hat{F}_\upsilon\dot{X} - KS - \tilde{J}^T u, \tag{18}$$

in which J^T was replaced by $\hat{J}^T - \tilde{J}^T$. From *p4*, it is deduced that

$$M\ddot{X} + C\dot{X} + G + F_\upsilon\dot{X} - (M+\tilde{M})\dot{\nu} - (C+\tilde{C})\nu - (G+\tilde{G}) - (F_\upsilon+\tilde{F}_\upsilon)\dot{X} = M\dot{S} + CS - Y_m\tilde{\theta}_m, \tag{19}$$

where (17) was used and $\tilde{*} = \hat{*} - *$. Furthermore, from (13), we have

$$\tilde{J}^T u = \bigg(\sum_{i=1}^{\ell} Y_{k_i}\tilde{\theta}_{k_i}\bigg)u. \tag{20}$$

Therefore, (18) may be expressed as follows

$$M\dot{S} + CS + KS = Y_m\tilde{\theta}_m - \bigg(\sum_{i=1}^{\ell} Y_{k_i}\tilde{\theta}_{k_i}\bigg)u \tag{21}$$

By considering

$$V = \frac{1}{2}S^T M S + \frac{1}{2}\tilde{\theta}_m^T\Gamma^{-1}\tilde{\theta}_m + \sum_{i=1}^{\ell}\frac{\tilde{\theta}_{k_i}^2}{2\gamma_i} \tag{22}$$

as a Lyapunov candidate, its derivative is

$$\dot{V} = S^T M\dot{S} + \frac{1}{2}S^T\dot{M}S + \tilde{\theta}_m^T\Gamma^{-1}\dot{\tilde{\theta}}_m + \sum_{i=1}^{\ell}\frac{\tilde{\theta}_{k_i}\dot{\tilde{\theta}}_{k_i}}{\gamma_i} \tag{23}$$

Authorized licensed use limited to: University of York. Downloaded on April 06,2025 at 12:25:52 UTC from IEEE Xplore. Restrictions apply.

in which $\dot{\tilde{\theta}} = \dot{\hat{\theta}}$ since θ is constant. By substituting $M\dot{S}$ from (21) and using *p1*, it is straightforward to show that

$$\dot{V} = -S^T K S. \tag{24}$$

Thus, asymptotic stability of the closed-loop system is achieved. Hence, in comparison with previous methods [24], [25], [26], the stability analysis of (16) is quite simple. □

Remark 2: In (1), similar to many articles, we did not model static friction. The reason is the fact that chiefly the desired trajectory is designed such that the robot is in motion all the time. Hence, in this situation, static friction is negligible. However, if the term $F_s \mathrm{sign}(\dot{X})$ that denotes the static friction is added to (1), we may simply modify the control law to ensure asymptotic stability. By this means, the terms $\hat{\mathcal{J}}\hat{F}_s \mathrm{sign}(\nu + \dot{X}_d)$ and $\hat{\mathcal{J}}\hat{F}_s \mathrm{sign}(\dot{X})$ are added to (10) and (16), respectively. Note that the stability proof is obvious since it is based on the singular perturbation method. □

Remark 3: In *Theorem 1*, it was shown that $\ddot{\tilde{X}}, \dot{\tilde{X}}, \tilde{X}$ and ν converge to zero. Replacing these values in the closed-loop equations, it is inferred that

$$\sum_{i=1}^{\ell} Y_{k_i}\tilde{\theta}_{k_i} \to 0, \qquad Y_m\tilde{\theta}_m \to 0. \tag{25}$$

However, the above equation does not necessarily lead to convergence of the estimated parameters to actual ones. Here, sufficient conditions of convergence of the estimated parameters to actual values are investigated. The first term of (25) may be interpreted as a summation of some weighted matrices. Therefore, if there exist no scalars υ_is such that

$$\sum_{i=1}^{\ell} \upsilon_i Y_{k_i} = 0, \tag{26}$$

then it is deduced that $\tilde{\theta}_{k_i} \to 0$. In the second term of (25), generally, we may argue that $\tilde{\theta}_m \in \ker\{Y_m\}$ where $\ker\{Y_m\}$ denotes the null space of Y_m. Thus, $\tilde{\theta}_m \to 0$ if Y_m is full column rank, or equivalently, $Y_m^T Y_m$ is full column rank. Note that both of the above conditions should satisfy simultaneously to ensure correct estimation of parameters. Notice that these results are given from theory perspective and are satisfied very nice in simulation. However, in practice, it highly depends on correct and comprehensive modeling of the system. □

As discussed before, assurance of positive tension in CDPMs is essential. Although the suitable design of the desired trajectory inside the robot's workspace is critical, usually a force distribution is also required in redundant CDPMs. In the literature, several methods have been developed to ensure tensile force in cables; see, for example, [33] and [34]. Invoking these articles, in the following remark, a method is introduced.

Remark 4: In the case of CDPMs, assume that the control law $u = u_0 + \bar{J}\aleph$ should be in the following range

$$0 \le u_{min} \le u_0 + \bar{J}\aleph \le u_{max}, \tag{27}$$

where u_{min} and u_{max} are vectors representing the lower and upper bounds of cable force, respectively, and u_0 denotes the first part of control law which is independent of $\bar{J}$.

Fig. 1. Description of determination of $\aleph$.

Now for simplicity, consider a fully-constrained CDPM with $m = n + 1$ that results in $\aleph$ and $\bar{J}$ being a scalar and a vector, respectively. In this case, if the robot is in the wrench-closure workspace, then all elements of $\bar{J}$ have the same sign [32], and (27) may be rewritten as

$$\begin{cases} \frac{u_{min_i} - u_{0_i}}{\bar{J}_i} \le \aleph \le \frac{u_{max_i} - u_{0_i}}{\bar{J}_i}, & \bar{J}_i > 0 \\ \frac{u_{min_i} - u_{0_i}}{\bar{J}_i} \ge \aleph \ge \frac{u_{max_i} - u_{0_i}}{\bar{J}_i}, & \bar{J}_i < 0 \end{cases}, \text{for } i = 1, \ldots, m \tag{28}$$

in which $\bar{J}_i$ denotes ith element of $\bar{J}$. From (28), a set of $\aleph_{min_i}$s and $\aleph_{max_i}$s are derived. By defining $\aleph_m = \max\{\aleph_{min_i}\}$ and $\aleph_M = \min\{\aleph_{max_i}\}$, we have

$$\aleph = \frac{\mu_1\aleph_m + \mu_2\aleph_M}{\mu_1 + \mu_2}, \qquad \mu_1, \mu_2 > 0 \qquad \mu_1 + \mu_2 = 1. \tag{29}$$

Fig. 1 shows a graphical description of the method. □

Discussion: In this section, the procedure of designing an adaptive controller was proposed. One may simply verify that the proposed methodology is much easier and more practical compared to previous works [24], [25]. Furthermore, the implementation of the controller is much simpler than that in [24] and [25], in which four sets of regressor forms have been considered. More precisely, the number of adaptation laws in [24] and [25] is

$$\begin{aligned} &a + a \cdot m \cdot l + b \cdot \mathfrak{c} + \mathfrak{c}, \\ &\times l \cdot m + a + b + \mathfrak{c}, \end{aligned} \tag{30}$$

respectively, while the number of adaptation laws of the proposed method is

$$\mathfrak{c} + \ell, \tag{31}$$

where $\mathfrak{c}, l$ and ℓ are determined in (4), (5) and (13), respectively, and a and b are defined in [25]. Recall that based on *p5*, it is inferred that $\ell \ll l$. Thus, the number of adaptation laws is obviously reduced. Note that the results of [26] are not mathematically well proven; see remark 1 of [25] for more details.

In order to test the proposed controllers in practice, two different-type of parallel robots are considered. First, the method is implemented on a flexible link robot and then, a rigid link parallel robot with a complex structure is considered. The results are proposed in the following section.

IV. Experimental Results

A. Cable-Driven Robot

The mechanism which is called Kamal-ol-molk robot, is a fully constraint CDPM whose end-effector is controlled via three single-phase motors through the cables. The robot has

Authorized licensed use limited to: University of York. Downloaded on April 06,2025 at 12:25:52 UTC from IEEE Xplore. Restrictions apply.

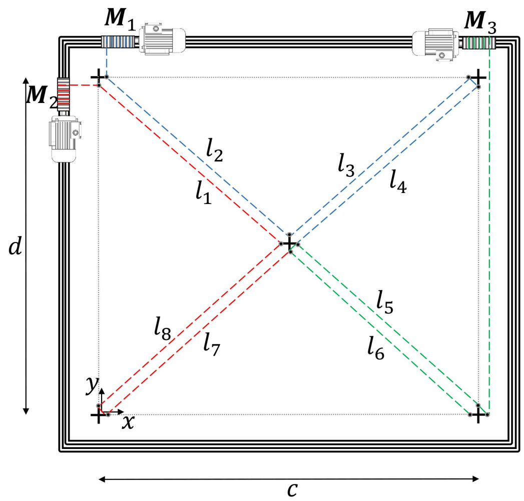

Fig. 2. Schematic of the cable-driven robot with parallelogram structure.

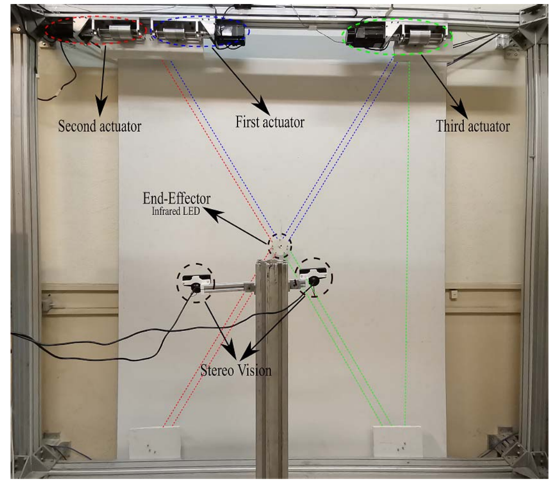

Fig. 3. Various parts of Kamal-ol-molk painter robot.

two transitional degrees of freedom in a vertical plane. The actuators can provide nominal torque 24.4 $Kg.cm$ and the radius of drums is $3cm$. Therefore, they sustain the maximum force equal to $80N$. Furthermore, all actuators are attached to the incremental non-contact optical encoder with an accuracy of about $30000ppr$. A schematic of the robot is depicted in Fig. 2. As indicated in this figure, in contrast to typical CDPMs, each actuator directly controls the length of at least two cables. Additionally, the structure of cables' connection from the end-effector to the constant points is in such a way that every two cables form a parallelogram. Although implementation of this structure is more complex than the traditional case, it may enlarge the workspace of the robot and also prevent pesky rotations of the end-effector. The curious reader is referred to [35] for more information about the structure.

With the purpose of measurement of cables' length, incremental encoders are used such that by knowing the initial value of cables, l_is are simply derived. Furthermore, a $100 frame/sec$ stereo vision camera is used to measure the position of the end-effector. Fig. 3 depicts different elements of the Kamal-ol-molk painter robot.

Dynamic equation of the manipulator under the assumption that cables are mass-less and infinitely stiff is as (1) with

$$M = \mathfrak{m} I_2, \quad C = 0, \quad G = [0, mg]^T, \quad F_v = 0, \tag{32}$$

where $\mathfrak{m}$ denotes the end-effector's mass, $X = [x, y]^T$ and the effects of natural damping terms are passed up. The Jacobian matrix of the robot is

$$J^T = -\begin{bmatrix} \frac{x}{l_2} + \frac{x-c}{l_3} + \frac{x-c}{l_4} & \frac{x}{l_1} + \frac{x}{l_7} + \frac{x}{l_8} & \frac{x-c}{l_5} + \frac{x-c}{l_6} \\ \frac{y-d}{l_2} + \frac{y-d}{l_3} + \frac{y-d}{l_4} & \frac{y-d}{l_1} + \frac{y}{l_7} + \frac{y}{l_8} & \frac{y}{l_5} + \frac{y}{l_6} \end{bmatrix} \tag{33}$$

with

$$\begin{aligned} &l_1^2 = l_2^2 = x^2 + (y-d)^2, \quad l_3^2 = l_4^2 = (x-c)^2 + (y-d)^2, \\ &l_5^2 = l_6^2 = (x-c)^2 + y^2, \quad l_7^2 = l_8^2 = x^2 + y^2, \end{aligned} \tag{34}$$

in which c and d are shown in Fig. 2. Due to the structure of the robot, the Jacobian matrix is not exactly matched with (6). However, invoking (6), we represent $J^T = -J_{new}^T L^{-1}$ with the following matrices

$$\begin{aligned} J_{new}^T &= \begin{bmatrix} l_3 x + 2l_2(x-c) & l_7 x + 2l_2 x & 2(x-c) \\ (l_3 + 2l_2)(y-d) & l_7(y-d) + 2l_2 y & 2y \end{bmatrix}, \\ L &= \mathrm{diag}\{l_2 l_3, l_2 l_7, l_5\}. \end{aligned} \tag{35}$$

Now, similar to (13), we have

$$\begin{aligned} J_{new}^T = &\begin{bmatrix} l_3 x + 2l_2 x & l_7 x + 2l_2 x & 2x \\ (l_3 + 2l_2) y & l_7 y + 2l_2 y & 2y \end{bmatrix} \\ &+ c\begin{bmatrix} -2l_2 & 0 & -2 \\ 0 & 0 & 0 \end{bmatrix} \\ &+ d\begin{bmatrix} 0 & 0 & 0 \\ -(l_3 + 2l_2) & -l_7 & 0 \end{bmatrix}. \end{aligned} \tag{36}$$

Furthermore, from (11), regressor of dynamic equation is as follows:

$$\mathfrak{m}\ddot{X}_d + m[0, g]^T = (\ddot{X}_d + [0, g]^T)\mathfrak{m} = Y_m \theta_m. \tag{37}$$

From the above equations, it is deduced that the number of unknown parameters and adaptation laws are equivalent. In other words, the values of the parameters in (30) are

$$a = 6, \quad b = 1, \quad \mathfrak{c} = 1, \quad l = 6, \quad \ell = 2, \tag{38}$$

that shows a significant improvement in lowering the number of adaptation laws.

The nominal values of the parameters of the robot are

$$\mathfrak{m} = 0.25Kg, \qquad c = 2.16m, \qquad d = 1.8m \tag{39}$$

A suitable desired trajectory similar to "design of ∞" is considered as follows:

$$x_d(t) = 1 - 0.2\cos(\frac{2\pi}{5}t), \quad y_d(t) = 0.82 + 0.1\sin(\frac{4\pi}{5}t). \tag{40}$$

The gains of the proposed controller in *Theorem 1* are set to

$$K_1 = 10I, \quad K_2 = 50I, \quad \Gamma = 5, \quad \gamma_1 = \gamma_2 = 2, \tag{41}$$

Authorized licensed use limited to: University of York. Downloaded on April 06,2025 at 12:25:52 UTC from IEEE Xplore. Restrictions apply.

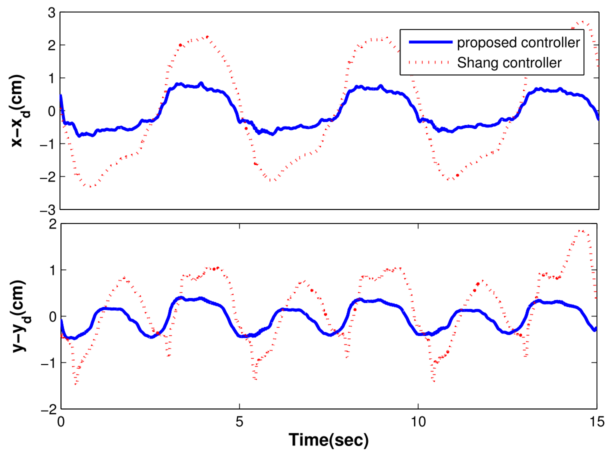

Fig. 4. The error of trajectory tracking of Kamal-ol-molk robot. Solid blue and dotted red are related to the proposed controller and Shang's controller in [26], respectively.

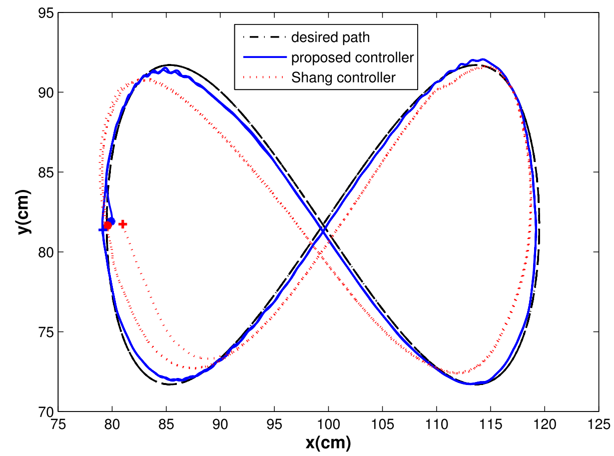

Fig. 5. The traversed and desired path of the robot. Apparently, the response of the proposed method is much better than the other given in [26]. The starting points and the ending points are illustrated with '$*$' and '$+$', respectively.

with $\rho = 0.1$ and $\epsilon = 0.01$. Furthermore, to compare the results, Shang's controller proposed in [26] is also implemented with the following gains

$$K_s = 0.5I,\ P = 10,\ \Gamma_k = 0.6I,\ \Gamma_d = I. \tag{42}$$

The parameters are perturbed about 10% and similar to [24] and [25], a simple projection algorithm is added to both controllers to confine the estimated parameters in the range of 15%.

The results are illustrated in Figs. 4-6. Fig. 4 shows the tracking errors of the controllers. As indicated in this figure, the tracking error of x and y with the proposed method is about $1cm$ and $0.5cm$, respectively, while it is $2cm$ and $1cm$ with the adaptive controller proposed in [26]. Furthermore, the error with the proposed method is damping gradually due to the adaptation of the parameters while it seems that $X - X_d$ is becoming larger with [26]. The reason is some mathematical drawbacks in the design and stability analysis of [26] (see Remark 1 of [25] for more details). The traversed path is shown in Fig. 5. It is clear that the path with the proposed controller is very close to the desired path. Recall that these results are derived while merely position is measured.

By considering the results on one hand, and the simplicity of the design on the other hand, the superiority of the proposed method is apparent. Fig. 6 shows the control signals of the controllers. The control efforts of *Theorem 1* are positive and less than $u_{max} = 80N$ due to the design of $\aleph$ based on Remark 4. Note that the reason why the control efforts of the methods are not quite matched is the use of different force distribution algorithms and also diverse tracking errors.

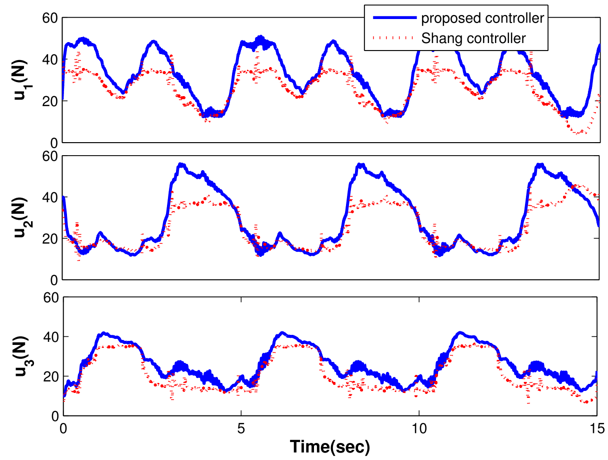

Fig. 6. Control signals of the controllers implemented on Kamal-ol-molk robot. Using the force distribution given in Remark 4, positive tension is ensured.

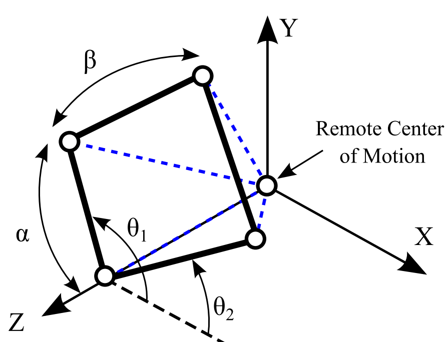

Fig. 7. Schematic of ARAS-Diamond.

B. Intraocular Surgery Robot

In order to examine the performance of the proposed controller based on the new representation (13) on a rigid link manipulator, the ARAS-Diamond robot is considered. ARAS-Diamond is a 2-DOF spherical parallel robot which was developed for minimally invasive eye surgery. As shown in Fig.7, the mechanism is a spherical parallel robot that consists of four interconnected links while all of them have a rotational motion around the remote center of motion (RCM) [36]. Fig. 8 illustrates the robot and its different parts.

In this robot, task-space variables are defined as $X = [\phi, \gamma]^T$ in the spherical coordinate system, while $\theta = [\theta_1, \theta_2]^T$ denotes joint variables. Moreover, angles $\alpha = \pi/4$ and $\beta = \pi/4$ are the geometric parameters of the robot. In [37], the

Authorized licensed use limited to: University of York. Downloaded on April 06,2025 at 12:25:52 UTC from IEEE Xplore. Restrictions apply.

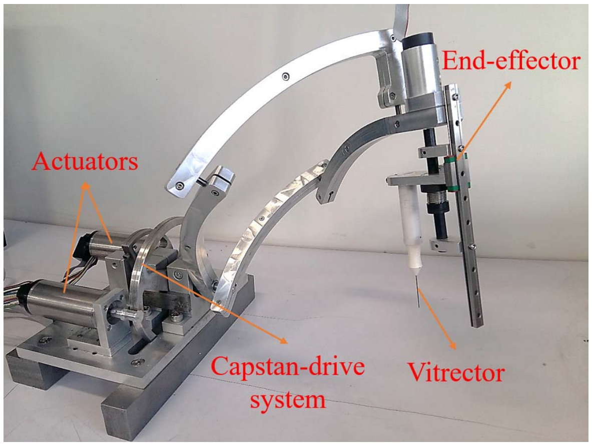

Fig. 8. ARAS-Diamond robot [36].

complete kinematic analysis of the robot is examined, and in this paper, only a short review is given. The Jacobian transpose of the robot is

$$J^T = \begin{bmatrix} 1 & 1 \\ \xi & -\xi \end{bmatrix}, \quad \xi = \frac{\theta_k - \cos \hat{A} \cot \gamma}{\sin \hat{A}}, \quad \hat{A} = \frac{\theta_1 - \theta_2}{2}, \tag{43}$$

where $\gamma, \theta_1, \theta_2$ are measured and $\theta_k = \cot \alpha$ is the unknown kinematic parameter. The transpose of Jacobian matrix is rewritten in the following form:

$$J^T = \begin{bmatrix} 1 & 1 \\ \frac{-\cos \hat{A} \cot \gamma}{\sin \hat{A}} & \frac{\cos \hat{A} \cot \gamma}{\sin \hat{A}} \end{bmatrix} + \begin{bmatrix} 0 & 0 \\ \frac{1}{\sin \hat{A}} & -\frac{1}{\sin \hat{A}} \end{bmatrix} \theta_k. \tag{44}$$

Invoking [38], [39], the explicit dynamic formulation (1) may be derived with the following parameters

$$\begin{aligned} M(X) &= \sum_{i=1}^{4} J_{\omega_i}{}^T \, {}^0 I_{A_i} \; J_{\omega_i}, \\ C(X, \dot{X}) &= \sum_{i=1}^{4} J_{\omega_i}{}^T \big({}^0 I_{A_i} J_{\omega_i} + (J_{\omega_i} \dot{X})_\times \, {}^0 I_{A_i} J_{\omega_i} \big), \\ G(X) &= -\sum_{i=1}^{4} m_i J_{\omega_i}{}^T \left({}^0 R_i \; {}^i \rho_{i\times} \; {}^0 R_i{}^T \right) g, \end{aligned} \tag{45}$$

in which, $(*)_\times \in \mathbb{R}^{3\times3}$ is skew-symmetric matrix representation of the vector $*$, and J_{ω_i} and ${}^0R_i$ represent Jacobian matrix and rotation matrix of each link, respectively. Moreover, ${}^0 I_{A_i}$ is the moment of inertia (MI) matrix of each link about the RCM point expressed in the base coordinate system, and $m_i \; {}^i \rho_i$ is the first moment (FM) of each link with respect to its center of gravity.

To derive regressor form $Y_m \theta_m$ for ARAS-Diamond, invoking [38], [39], θ_m is derived as follows:

$$\begin{aligned} \theta_m &= [\theta_{m_1}, \theta_{m_2}, \theta_{m_3}, \theta_{m_4}]^T \in \mathbb{R}^{36\times1} \\ \theta_{m_i} &= \left[m_i \; {}^i \rho_i, {}^i \bar{I}_{A_i} \right]^T, \qquad i \in \{1, \ldots, 4\}, \end{aligned} \tag{46}$$

in which, ${}^i \bar{I}_{A_i}$ denotes linear form of inertia matrix of each link and defined as

$${}^i \bar{\mathrm{I}}_{A_i} = [I_{xx_{A_i}}, I_{xy_{A_i}}, I_{xz_{A_i}}, I_{yy_{A_i}}, I_{yz_{A_i}}, I_{zz_{A_i}}]^T. \tag{47}$$

TABLE II
NOMINAL PARAMETERS OF ARAS-DIAMOND. ALL THE UNITS ARE SI

Symbol	Description	Value
$m_1 \; {}^1\rho_1$	FM 1	$[0.011, 0, 0.027]^T$
$m_2 \; {}^2\rho_2$	FM 2	$[0.009, 0, 0.023]^T$
$m_3 \; {}^3\rho_3$	FM 3	$[0.016, 0, 0.039]^T$
$m_4 \; {}^4\rho_4$	FM 4	$[0.011, 0, 0.027]^T$
${}^1 I_1$	MI 1	$diag(6.440, 6.350, 1.716)10^{-4}$
${}^2 I_2$	MI 2	$diag(5.359, 5.284, 0.150)10^{-4}$
${}^3 I_3$	MI 3	$diag(9.849, 9.342, 0.610)10^{-4}$
${}^4 I_4$	MI 4	$diag(7.577, 7.496, 2.348)10^{-4}$
F_v	VF	$[0.034, 0.008]^T$

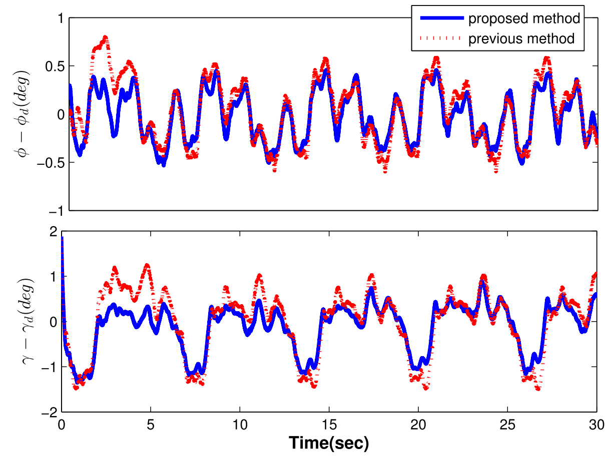

Fig. 9. The error of trajectory tracking of ARAS Diamond robot based on the controller of Remark 1 and proposed method in [25].

The nominal values of the robot's parameters are reported in Table II. The desired trajectory is

$$\phi_d(t) = \pi/9 \sin(t) + \pi/2, \qquad \gamma_d(t) = \pi/9 sin(t) + \pi/3. \tag{48}$$

The kinematic and dynamic parameters are perturbed about 10% and 20%, respectively. To justly compare the results, the controller (16) in Remark 1 with the following gains

$$K = 4I, \quad \Pi = 8I, \quad \Gamma = I, \quad \gamma_1 = 3. \tag{49}$$

together with the proposed method in [25] with the following gains

$$\begin{aligned} &K_1 = 4I, \; K_2 = 4I, \; K_3 = 3I, \; \Gamma = 20I, \; \Gamma' = 20I, \\ &A = 25I, \; C = 15I, \; D = 15I, \; F = 20I, \end{aligned} \tag{50}$$

which both of them are based on Slotine and Li controller, are implemented on the robot. The results are depicted in Fig. 9 and Fig. 10. As indicated in Fig. 9, the steady-state error of both controllers is small and negligible. However, the steady-state error of the proposed controller is slightly smaller than that reported in [25]. Furthermore, in the initial times, it is apparent that the proficiency of the proposed method is much better. It is due to the fact that the number of adaptations in [25] is excessively more than that of the proposed controller.

Authorized licensed use limited to: University of York. Downloaded on April 06,2025 at 12:25:52 UTC from IEEE Xplore. Restrictions apply.

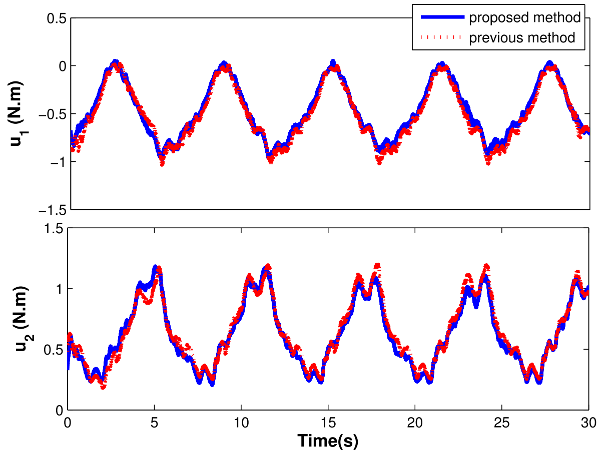

Fig. 10. Control efforts of ARAS Diamond.

TABLE III
RMS AND ITAE OF ERRORS OF ARAS-DIAMOND

Controller	Criterion	ϕ	γ
Ref. [25]	RMS	0.3326	0.7327
Proposed controller	RMS	0.2593	0.5402
Ref. [25]	ITAE	123.8	247.1
Proposed controller	ITAE	99.5	177.9

To better compare the results, the root mean square (RMS) and the integral time absolute error (ITAE) of errors are shown in Table III. It is clear that the RMS related to the proposed controller is almost half of the other and also the ITAE of proposed method is less than the ITAE of [25]. Thus, we can conclude that the method is not only simple to be implemented but also performs well. Note that we use RMS and ITAE since they are well-known indexes. It is clear that if we use other indexes, same results, i.e., superiority of the proposed method, are obtained. Fig. 10 shows the control efforts of the controllers. Since u_is of both controllers pettily differ, it is deduced that slight variations may lead to significant improvement.

At the end of this section, it is good to mention that the disadvantages of the proposed method (similar to a general adaptive controller) is the requirement of representation of the expressions in regressor form and also the inability to suppress or reduce the effects of external disturbance/unmodeled dynamics. Note that the former is accessible in most cases, but there is not a general method to derive it, and the latter may be addressed by adding a robust controller such as H_2 or H_∞ in the outer loop to reduces the effects of external disturbance.

V. Conclusion and Future Prospects

In this article, an adaptive trajectory tracking controller for parallel manipulators in the presence of uncertain dynamic and kinematic parameters with merely position feedback was proposed. It was shown that by the suitable representation of the Jacobian matrix in regressor form, the number of adaptation laws reduces, while the stability of the closed-loop system was guaranteed by a suitable Lyapunov candidate. Furthermore, the effects of the right kernel of the Jacobian matrix in control law were analyzed, such that tensile forces in cable-driven manipulators are guaranteed. The results were verified and compared to previous methods through some experiments. Future research is being conducted on modification and applying the proposed method to serial robots. Furthermore, designing a robust adaptive controller to reduce the effects of disturbance is underway.

Appendix
Proof of *Theorem 1*

Substitute (10) in (1), the closed-loop equations are

$$\begin{aligned} M\ddot{X} + C(X,\dot{X})\dot{X} + G + F_v\dot{X} &= J^T\hat{\mathcal{J}}\Big(\hat{M}\ddot{X}_d \\ &\quad + \hat{C}(X,\dot{X}_d)\dot{X}_d + \hat{G} + \hat{F}_v\dot{X}_d - K_1\nu - K_2\tilde{X}\Big) \\ &\quad + J^T\hat{\bar{J}}\aleph = \left(\sum_{i=1}^{\ell} Y_{k_i}\theta_{k_i}\right)\hat{\mathcal{J}}\Big(\hat{M}\ddot{X}_d + \hat{C}(X,\dot{X}_d)\dot{X}_d \\ &\quad + \hat{G} + \hat{F}_v\dot{X}_d - K_1\nu - K_2\tilde{X}\Big) + \left(\sum_{i=1}^{\ell} Y_{k_i}\theta_{k_i}\right)\hat{\bar{J}}\aleph, \end{aligned} \tag{51}$$

Substitute $\theta_{k_i} = \hat{\theta}_{k_i} - \tilde{\theta}_{k_i}$ and considering this facts that

$$\left(\sum_{i=1}^{\ell} Y_{k_i}\hat{\theta}_{k_i}\right)\hat{\mathcal{J}} = I_n, \qquad \left(\sum_{i=1}^{\ell} Y_{k_i}\hat{\theta}_{k_i}\right)\hat{\bar{J}} = 0, \tag{52}$$

then (51) is as follows

$$\begin{aligned} M\ddot{X} + C(X,\dot{X})\dot{X} + G + F_v\dot{X} &= \Big(\hat{M}\ddot{X}_d + \hat{C}(X,\dot{X}_d)\dot{X}_d \\ &\quad + \hat{G} + \hat{F}_v\dot{X}_d - K_1\nu - K_2\tilde{X}\Big) + \left(\sum_{i=1}^{\ell} Y_{k_i}\tilde{\theta}_{k_i}\right)\Big(\hat{\mathcal{J}}\big(\hat{M}\ddot{X}_d \\ &\quad + \hat{C}(X,\dot{X}_d)\dot{X}_d + \hat{G} + \hat{F}_v\dot{X}_d - K_1\nu - K_2\tilde{X}\big) + \hat{\bar{J}}\aleph\Big) \end{aligned} \tag{53}$$

From (11), it is deduced that

$$\begin{aligned} &\hat{M}\ddot{X}_d + \hat{C}(X,\dot{X}_d)\dot{X}_d + \hat{G} + \hat{F}_v\dot{X}_d = M\ddot{X}_d + C(X,\dot{X}_d) \\ &\quad \times \dot{X}_d + G + F_v\dot{X}_d + \tilde{M}\ddot{X}_d + \tilde{C}(X,\dot{X}_d)\dot{X}_d + \tilde{G} + \tilde{F}_v\dot{X}_d \\ &= M\ddot{X}_d + C(X,\dot{X}_d)\dot{X}_d + G + F_v\dot{X}_d + Y_m(\ddot{X}_d,\dot{X}_d,X)\tilde{\theta}_m. \end{aligned} \tag{54}$$

Therefore, (53) is in the following form

$$\begin{aligned} M\ddot{\tilde{X}} &= -C(X,\dot{X})\dot{\tilde{X}} - C(X,\dot{X}_d)\dot{\tilde{X}} - F_v\dot{\tilde{X}} - K_1\nu \\ &\quad - K_2\tilde{X} + \left(\sum_{i=1}^{\ell} Y_{k_i}\tilde{\theta}_{k_i}\right)\Big(\hat{\mathcal{J}}\big(\hat{M}\ddot{X}_d + \hat{C}(X,\dot{X}_d)\dot{X}_d \\ &\quad \times \hat{G} + \hat{F}_v\dot{X}_d - K_1\nu - K_2\tilde{X}\big) + \hat{\bar{J}}\aleph\Big) + Y_m\tilde{\theta}_m, \end{aligned} \tag{55}$$

where $p2$ was used. Furthermore, from (8), it is deduced that

$$\epsilon\dot{\nu} = -\nu + \dot{\tilde{X}}, \tag{56}$$

with $\epsilon = 1/\delta$. Thus, the collections of closed-loop equations are (14), (53) and (56).

Authorized licensed use limited to: University of York. Downloaded on April 06,2025 at 12:25:52 UTC from IEEE Xplore. Restrictions apply.

To analyze the stability, we invoke the singular perturbation method [40, ch. 9] (see also [28]). First, by setting $\epsilon = 0$ in (56), the quasi steady state solution is $\nu = \dot{\tilde{X}}$. Replacing ν in (14) and (53) by $\dot{\tilde{X}}$, the dynamic of the reduced system is obtained. To analyze its stability, the following Lyapunov candidate is considered

$$\begin{aligned} V &= V_1 + V_2 \\ V_1 &= \frac{1}{2}\dot{\tilde{X}}^T M \dot{\tilde{X}} + \frac{1}{2}\tilde{X}^T K_2 \tilde{X} + \rho \dot{\tilde{X}} M \tanh(\tilde{X}) \\ V_2 &= \frac{1}{2}\tilde{\theta}_m^T \Gamma^{-1}\tilde{\theta}_m + \sum_{i=1}^{\ell} \frac{\tilde{\theta}_{k_i}^2}{2\gamma_i}. \end{aligned} \tag{57}$$

First, we should show that V_1 is a suitable Lyapunov candidate. Hence,

$$\begin{aligned} V \geq\ & \frac{1}{2}\lambda_{min}\{M\}\|\dot{\tilde{X}}\|^2 + \frac{1}{2}\lambda_{min}\{K_2\}\|\tilde{X}\|^2 \\ & - \frac{\rho}{2}\lambda_{max}\{M\}\|\dot{\tilde{X}}\|^2 - \frac{\rho}{2}\lambda_{max}\{M\}\|\tilde{X}\|^2. \end{aligned} \tag{58}$$

Thus, (57) is a suitable Lyapunov function under the following conservative condition

$$\rho < \min\left\{\frac{\lambda_{min}\{M\}}{\lambda_{max}\{M\}}, \frac{\lambda_{min}\{K_2\}}{\lambda_{max}\{M\}}\right\} \tag{59}$$

The derivative of (57) along the trajectories of the system by replacing $\nu = \dot{\tilde{X}}$ is

$$\begin{aligned} \dot{V} =\ & \left(\dot{\tilde{X}}^T + \rho \tanh^T(\tilde{X})\right)\Bigg\{-C(X,\dot{X})\dot{\tilde{X}} - C(X,\dot{X}_d)\dot{\tilde{X}} \\ & - F_v\dot{\tilde{X}} - K_1\nu - K_2\tilde{X} + \left(\sum_{i=1}^{\ell} Y_{k_i}\tilde{\theta}_{k_i}\right)\Bigg[\hat{\mathcal{J}}\Bigg(Y_m\hat{\theta}_m - K_1\nu \\ & - K_2\tilde{X}\Bigg) + \hat{J}\aleph\Bigg] + Y_m\tilde{\theta}_m\Bigg\} + \frac{1}{2}\dot{\tilde{X}}^T \dot{M}\dot{\tilde{X}} + \dot{\tilde{X}}^T K_2\tilde{X} \\ & + \rho\dot{\tilde{X}}^T M \mathrm{sech}^2(\tilde{X})\dot{\tilde{X}} + \dot{\tilde{\theta}}_m^T\Gamma^{-1}\tilde{\theta}_m + \sum_{i=1}^{\ell}\frac{\tilde{\theta}_{k_i}\dot{\tilde{\theta}}_{k_i}}{\gamma_i}. \end{aligned} \tag{60}$$

Using *p1-p3* and replacing the adaptation laws, the upper bound of $\dot{V}$ is

$$\begin{aligned} \dot{V} \leq\ & \left(\kappa_c\kappa_{\dot{X}_d} - f_{v_{min}} - \lambda_{min}\{K_1\} + \rho\kappa_c\sqrt{n} + \rho\lambda_{max}\{M\}\right) \\ & \times \|\dot{\tilde{X}}\|^2 + \left(2\rho\kappa_c\kappa_{\dot{X}_d} + \rho f_{v_{max}} + \rho\lambda_{max}\{K_1\}\right) \\ & \times \|\dot{\tilde{X}}\|\|\tanh(\tilde{X})\| \\ & - \rho\lambda_{min}\{K_2\}\|\tanh(\tilde{X})\|^2 = -\zeta^T Q\zeta^T \end{aligned} \tag{61}$$

with $\zeta = [\|\tanh(\tilde{X})\|, \|\dot{\tilde{X}}\|]^T$ and Q is as follows

$$\begin{bmatrix} \rho\lambda_{min}\{K_2\} & \begin{matrix} -\rho\kappa_c\kappa_{\dot{X}_d} - \frac{\rho f_{v_{max}}}{2} \\ -\frac{\rho\lambda_{max}\{K_1\}}{2} \end{matrix} \\ \begin{matrix} -\rho\kappa_c\kappa_{\dot{X}_d} - \frac{\rho f_{v_{max}}}{2} \\ -\frac{\rho\lambda_{max}\{K_1\}}{2} \end{matrix} & \begin{matrix} -\kappa_c\kappa_{\dot{X}_d} + f_{v_{min}} \\ +\lambda_{min}\{K_1\} - \rho\kappa_c\sqrt{n} \\ -\rho\lambda_{max}\{M\} \end{matrix} \end{bmatrix} \tag{62}$$

where $\|\dot{X}_d\| \leq \kappa_{\dot{X}_d}$ was used. In order to have $Q > 0$, ρ should be selected such that

$$\rho < \min\left\{\frac{-\kappa_c\kappa_{\dot{X}_d} + \lambda_{min}\{K_1\} + f_{v_{min}}}{\kappa_c\sqrt{n} + \lambda_{max}\{M\}}\right\}. \tag{63}$$

Now, we shall analyze the dynamic of boundary layer (56) in which $\dot{\tilde{X}}$ is construed as a constant. It is clear that the term $-\nu + \dot{\tilde{X}}$ converges exponentially fast to zero. The proof is completed if the dynamic of the observer (56) is sufficiently faster than closed-loop system's dynamic. A conservative upper bound of ϵ is derived from [40, ch. 9] as follows

$$\begin{aligned} \epsilon &< \frac{c_1 c_3}{c_2 c_4} \\ c_1 &= \min\left\{\frac{\lambda_{min}\{M\} - \rho\lambda_{max}\{M\}}{2}, \frac{\lambda_{min}\{K_2\} - \rho\lambda_{max}\{M\}}{2}\right\} \\ c_2 &= \max\left\{\frac{\lambda_{max}\{M\} + \rho\lambda_{max}\{M\}}{2}, \frac{\lambda_{max}\{K_2\} + \rho\lambda_{max}\{M\}}{2}\right\} \\ c_3 &= \lambda_{min}\{Q\} \\ c_4 &= \max\left\{(1+\rho)\lambda_{max}\{M\} + \rho\kappa_c, \lambda_{max}\{K_2\} + \rho\lambda_{max}\{M\}\right\}. \end{aligned} \tag{64}$$

References

[1] A. Abbasi, S. MahmoudZadeh, and A. Yazdani, "A cooperative dynamic task assignment framework for COTSBot AUVs," *IEEE Trans. Autom. Sci. Eng.*, vol. 19, no. 2, pp. 1163–1179, Apr. 2022.

[2] X. Yu, W. He, Q. Li, Y. Li, and B. Li, "Human-robot co-carrying using visual and force sensing," *IEEE Trans. Ind. Electron.*, vol. 68, no. 9, pp. 8657–8666, Sep. 2021.

[3] L. Schreiber and C. Gosselin, "Schönflies motion PARALLeL robot (SPARA): A kinematically redundant parallel robot with unlimited rotation capabilities," *IEEE/ASME Trans. Mechatronics*, vol. 24, no. 5, pp. 2273–2281, Oct. 2019.

[4] W. Shang, S. Cong, and Y. Ge, "Coordination motion control in the task space for parallel manipulators with actuation redundancy," *IEEE Trans. Autom. Sci. Eng.*, vol. 10, no. 3, pp. 665–673, Jul. 2013.

[5] M. R. J. Harandi, S. A. Khalilpour, and H. D. Taghirad, "Adaptive energy shaping control of a 3-DOF underactuated cable-driven parallel robot," *IEEE Trans. Ind. Informat.*, early access, Oct. 4, 2022, doi: 10.1109/TII.2022.3211980.

[6] E. Ida, S. Briot, and M. Carricato, "Natural oscillations of underactuated cable-driven parallel robots," *IEEE Access*, vol. 9, pp. 71660–71672, 2021.

[7] M. R. J. Harandi, "Passivity based control of 3-DOF underactuated suspended cable-driven robot," Ph.D. thesis, K. N. Toosi Univ. Technol., Tehran, Iran, 2021.

[8] M. R. J. Harandi, S. A. Khalilpour, and H. Taghirad, "Robust IDA-PBC for a spatial underactuated cable driven robot with bounded inputs," in *Proc. 29th Iranian Conf. Electr. Eng. (ICEE)*, May 2021, pp. 689–694.

[9] H. Yuan, X. You, Y. Zhang, W. Zhang, and W. Xu, "A novel calibration algorithm for cable-driven parallel robots with application to rehabilitation," *Appl. Sci.*, vol. 9, no. 11, p. 2182, May 2019.

[10] X. Huo, B. Lian, P. Wang, Y. Song, and T. Sun, "Dynamic identification of a tracking parallel mechanism," *Mechanism Mach. Theory*, vol. 155, Jan. 2021, Art. no. 104091.

[11] X. Yu, B. Li, W. He, Y. Feng, L. Cheng, and C. Silvestre, "Adaptive-constrained impedance control for human–robot co-transportation," *IEEE Trans. Cybern.*, vol. 52, no. 12, pp. 13237–13249, Dec. 2022.

[12] R. Ortega, V. Gromov, E. Nuño, A. Pyrkin, and J. G. Romero, "Parameter estimation of nonlinearly parameterized regressions without overparameterization: Application to adaptive control," *Automatica*, vol. 127, May 2021, Art. no. 109544.

[13] T. Yang, N. Sun, Y. Fang, X. Xin, and H. Chen, "New adaptive control methods for *n*-link robot manipulators with online gravity compensation: Design and experiments," *IEEE Trans. Ind. Electron.*, vol. 69, no. 1, pp. 539–548, Jan. 2022.

[14] M. I. Hosseini, M. J. Harandi, S. K. Seyedi, and H. Taghirad, "Experimental performance of adaptive fast terminal sliding mode control on a suspended cable robot," *J. Electr. Comput. Eng. Innov.*, vol. 7, no. 1, pp. 57–66, 2019.

[15] R. Hao, J. Wang, J. Zhao, and S. Wang, "Observer-based robust control of 6-DOF parallel electrical manipulator with fast friction estimation," *IEEE Trans. Autom. Sci. Eng.*, vol. 13, no. 3, pp. 1399–1408, Jul. 2016.

[16] W. Shang, F. Xie, B. Zhang, S. Cong, and Z. Li, "Adaptive cross-coupled control of cable-driven parallel robots with model uncertainties," *IEEE Robot. Autom. Lett.*, vol. 5, no. 3, pp. 4110–4117, Jul. 2020.

Authorized licensed use limited to: University of York. Downloaded on April 06,2025 at 12:25:52 UTC from IEEE Xplore. Restrictions apply.

[17] W. Shang, B. Zhang, S. Cong, and Y. Lou, "Dual-space adaptive synchronization control of redundantly-actuated cable-driven parallel robots," *Mechanism Mach. Theory*, vol. 152, Oct. 2020, Art. no. 103954.

[18] M. R. J. Harandi and H. D. Taghirad, "Adaptive interconnection and damping assignment passivity-based control for an underactuated cable-driven robot," *Int. J. Adapt. Control Signal Process.*, vol. 35, no. 12, pp. 2487–2498, Dec. 2021.

[19] C. Sun et al., "Design and optimization of three-degree-of-freedom planar adaptive cable-driven parallel robots using the cable wrapping phenomenon," *Mechanism Mach. Theory*, vol. 166, Dec. 2021, Art. no. 104475.

[20] J.-J. E. Slotine and W. Li, "On the adaptive control of robot manipulators," *Int. J. Robot. Res.*, vol. 6, no. 3, pp. 49–59, 1987.

[21] D. Braganza, W. E. Dixon, D. M. Dawson, and B. Xian, "Tracking control for robot manipulators with kinematic and dynamic uncertainty," in *Proc. 44th IEEE Conf. Decis. Control*, Dec. 2005, pp. 5293–5297.

[22] C. C. Cheah, C. Liu, and J. J. E. Slotine, "Adaptive tracking control for robots with unknown kinematic and dynamic properties," *Int. J. Robot. Res.*, vol. 25, no. 3, pp. 283–296, 2006.

[23] H. Wang, "Adaptive control of robot manipulators with uncertain kinematics and dynamics," *IEEE Trans. Autom. Control*, vol. 62, no. 2, pp. 948–954, Feb. 2017.

[24] M. R. J. Harandi, S. A. Khalilpour, H. D. Taghirad, and J. G. Romero, "Adaptive control of parallel robots with uncertain kinematics and dynamics," *Mech. Syst. Signal Process.*, vol. 157, Aug. 2021, Art. no. 107693.

[25] M. R. J. Harandi, S. A. Khalilpour, and H. D. Taghirad, "Adaptive dynamic feedback control of parallel robots with unknown kinematic and dynamic properties," *ISA Trans.*, vol. 126, pp. 574–584, Jul. 2022.

[26] H. Ji, W. Shang, and S. Cong, "Adaptive synchronization control of cable-driven parallel robots with uncertain kinematics and dynamics," *IEEE Trans. Ind. Electron.*, vol. 68, no. 9, pp. 8444–8454, Sep. 2021.

[27] J. G. Romero, R. Ortega, and I. Sarras, "A globally exponentially stable tracking controller for mechanical systems using position feedback," *IEEE Trans. Autom. Control*, vol. 60, no. 3, pp. 818–823, Mar. 2015.

[28] J. Moreno-Valenzuela, V. Santibá nez, and R. Campa, "On output feedback tracking control of robot manipulators with bounded torque input," *Int. J. Control, Autom., Syst.*, vol. 6, no. 1, pp. 76–85, 2008.

[29] N. Sun, Y. Fu, T. Yang, J. Zhang, Y. Fang, and X. Xin, "Nonlinear motion control of complicated dual rotary crane systems without velocity feedback: Design, analysis, and hardware experiments," *IEEE Trans. Autom. Sci. Eng.*, vol. 17, no. 2, pp. 1017–1029, Apr. 2020.

[30] Y. Su, P. C. Müller, and C. Zheng, "Global asymptotic saturated PID control for robot manipulators," *IEEE Trans. Control Syst. Technol.*, vol. 18, no. 6, pp. 1280–1288, Nov. 2010.

[31] M. R. J. Harandi, H. D. Taghirad, A. Molaei, and J. Guadalupe Romero, "Bounded inputs total energy shaping for a class of underactuated mechanical systems," *Int. J. Robust Nonlinear Control*, vol. 31, no. 18, pp. 9267–9281, Dec. 2021.

[32] H. D. Taghirad, *Parallel Robots: Mechanics and Control*. Boca Raton, FL, USA: CRC Press, 2013.

[33] M. R. J. Harandi, S. A. Khalilpour, H. Damirchi, and H. D. Taghirad, "Stabilization of cable driven robots using interconnection matrix: Ensuring positive tension," in *Proc. 7th Int. Conf. Robot. Mechatronics (ICRoM)*, Nov. 2019, pp. 235–240.

[34] S.-R. Oh and S. K. Agrawal, "Cable suspended planar robots with redundant cables: Controllers with positive tensions," *IEEE Trans. Robot.*, vol. 21, no. 3, pp. 457–465, Jun. 2005.

[35] N. Khodadadi, M. I. Hosseini, S. A. Khalilpour, H. D. Taghirad, and P. Cardou, "Multi objective optimization of a cable-driven robot with parallelogram links," in *Proc. Int. Conf. Cable-Driven Parallel Robots*. Cham, Switzerland: Springer, 2021, pp. 170–181.

[36] A. Bataleblu, R. Khorrambakht, and H. D. Taghirad, "Robust H_∞-based control of ARAS-diamond: A vitrectomy eye surgery robot," *Proc. Inst. Mech. Eng., C, J. Mech. Eng. Sci.*, vol. 235, no. 20, pp. 5116–5131, 2020.

[37] A. Molaei, E. Abedloo, H. D. Taghirad, and Z. Marvi, "Kinematic and workspace analysis of DIAMOND: An innovative eye surgery robot," in *Proc. 23rd Iranian Conf. Electr. Eng.*, May 2015, pp. 882–887.

[38] A. Hassani, A. Bataleblu, S. A. Khalilpour, H. D. Taghirad, and P. Cardou, "Dynamic models of spherical parallel robots for model-based control schemes," 2021, *arXiv:2110.00491*.

[39] M. R. J. Harandi, A. Hassani, S. Khalilpour, and H. D. Taghirad, "Practical adaptive position feedback regulator for parallel robots with bounded inputs," *J. Vib. Control*, early access, 2022, doi: 10.1177/10775463221083361.

[40] H. K. Khalil and J. Grizzle, *Nonlinear Systems*, vol. 3. Upper Saddle River, NJ, USA: Prentice-Hall, 2002.

M. Reza J. Harandi received the B.Sc. and M.Sc. degrees in control engineering from Sharif University, Tehran, Iran, in 2014 and 2016, respectively, and the Ph.D. degree in control engineering from K. N. Toosi University, Tehran, in 2021. His current research interests include various aspects, including stabilization of underactuated robots, adaptive control, passivity-based control, power systems, parallel, and cable-driven robots.

Ali Hassani received the B.Sc. degree in mechanical engineering from Shahid Chamran University, Ahvaz, Iran, in 2018, and the M.Sc. degree in mechatronics engineering from the Department of Electrical and Computer Engineering, K. N. Toosi University of Technology, Tehran, Iran, in 2022. He is currently a Researcher with the Advanced Robotics and Automated System (ARAS), K. N. Toosi University of Technology. His current research interests include medical robotics and robot-assisted surgery systems, parallel manipulators, and multibody system dynamics.

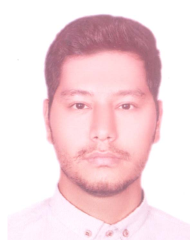

Mohammad Isaac Hosseini received the B.Sc. degree in electrical engineering from the Qom University of Technology, Qom, Iran, in 2017, and the M.Sc. degree in electrical engineering in the field of control engineering from K. N. Toosi University, Tehran, Iran, in 2021. He is currently an Assistant Researcher at the Advanced Robotics and Automated System (ARAS) Laboratory, K. N. Toosi University of Technology. His research interests include the study and analysis of nonlinear systems and control of parallel robots with particular emphasis on cable-driven robots.

Hamid D. Taghirad (Senior Member, IEEE) received the B.Sc. degree in mechanical engineering from the Sharif University of Technology, Tehran, Iran, in 1989, and the M.Sc. degree in mechanical engineering and the Ph.D. degree in electrical engineering from McGill University, Montreal, Canada, in 1993 and 1997, respectively. He is currently a Professor and the Director of the Advanced Robotics and Automated System (ARAS), Department of Systems and Control, Faculty of Electrical Engineering, K. N. Toosi University of Technology. He is also an Associate Editor of *Frontiers in Robotics and AI—Biomedical Robotics* and the Editorial Board of *International Journal of Advanced Robotic Systems*. His research interests include robust and nonlinear control applied to robotic systems. His publications include five books and more than 250 papers in international journals and conference proceedings.

Authorized licensed use limited to: University of York. Downloaded on April 06,2025 at 12:25:52 UTC from IEEE Xplore. Restrictions apply.